

A Tracking System Control Approach Applied on a Rotary Inverted Pendulum Model

Luiz Eduardo Pivovar*, Ricardo Breganon*, Uiliam Nelson Lendzion Tomaz Alves*, Fernando Sabino Fontequ Ribeiro*, Gustavo Vendrame Barbara*, João Paulo Lima Silva de Almeida* and Marcio Mendonça**

**(Federal Institute of Paraná, IFPR, Av. Dr. Tito, 801, Jacarezinho – PR, Brazil)*

***(Federal University of Technology of Paraná, UTFPR, Av. Alberto Carazzai, 1640, Cornélio Procópio – PR, Brazil)*

ABSTRACT

The rotary inverted pendulum (Furuta pendulum) is a didact equipment used for studying and applications of control techniques, since its model has non-linearities and unstable equilibrium point when the pendulum is in the vertical position. This paper presents the modelling of a mechanical structure of a rotary inverted pendulum and, using the linearization around the operation point, describes the design of a tracking system controller to this system, considering both state feedback or observed state feedback from a state observer. Results from simulations are presented based on two comparative cases, in which, in the first one only the tracking system controller is considered and, in the second one a state observer is added to the strategy. The results show that the proposed control strategies were able to lead the linear model to the equilibrium point, as well as allow the controlled output follow reference signals. Thus, the modelling and controlling methodologies have presented promising results.

Keywords-Rotary inverted pendulum, State observer, Tracking system controller.

Date of Submission: 18-05-2020

Date of Acceptance: 03-06-2020

I. INTRODUCTION

The rotary inverted pendulum is a classic mechanical system for the studying of the control techniques at laboratories. It was developed by Furuta [1, 2, 3], in 1992, and it consists of a system with two degrees of freedom, composed by two rotary joints. Its rotational movement is based on the torque application by a motor coupled on one of its joints. The interest in studying this system is due to its non-linear behavior, which is compared to several similar problems found in interesting industrial applications, such as spatial rockets, bipedal robots, satellite launchers and vehicles for individual transportation [4, 5].

In the literature, modelling and controlling strategies for the rotary inverted pendulum, usually known as Furuta pendulum, are widely widespread. Such strategies encompass from traditional industrial controllers (PID, PI, among others) [5] to more advanced control strategies, as described in the following. In [6], a predictive controller based on an optimal control law considering perturbation is presented. A linear regulating controller with state feedback, based on differential leveling and root allocation, is described in [7]. In [8], a linear quadratic regulator (LQR) approach is described. A

destabilizing controller that uses positive feedback is presented in [9]. A linear state feedback controller is presented in [10]. Among the intelligent control strategies, the fuzzy controllers are highlighted [11, 12, 13]. All the mentioned works consider the inverted pendulum stabilization in the vertical position.

Among the modern control techniques, in which they consider state space models, a tracking system control is highlighted. In this technique, a determined system's output must follow a reference signal [5, 14, 15]. However, this control approach requires the measurement of all state variables, which is not always feasible. In this case, it is possible to use a state observer in order to estimate all the state variables by means of the system's output measurements and, then, the tracking system controller can use the observed state to compose the control signal.

Considering a linear approximation of the system's mathematical model, around the point in which the pendulum position is vertical (inverted), the presented work describes the application of the tracking system control technique, with state feedback, to achieve a position control and stabilization of the rotary inverted pendulum. Due to the impossibility to measure all the state variables, a

state observer was also considered in the control loop. The results are evaluated considering the following comparative cases: (i) tracking system controller; and (ii) tracking system controller along with state observer.

The rest of this paper is organized as follows: in Section II, the main constructive characteristics of a Furuta pendulum are presented. In Section III, the system's linear mathematical model is discussed. A description about the considered control techniques is presented in Section IV, followed by the results and discussions, in the Section V, and by the main conclusions of the paper, in the Section VI.

II. ROTARY INVERTED PENDULUM: FURUTA PENDULUM

The rotary inverted pendulum is a didact equipment used for studying and applications of control techniques, mainly in Engineering courses, due to its non-linear characteristics and its unstable equilibrium point. These features allow experiments using advanced control approaches.

In general, the inverted pendulum is composed by a rotational arm (A) in which a DC motor (12V) is coupled at one of its extremity, as presented in Fig. 1. A torque (τ) is generated by means of the DC motor actioning, which provides the movement of the mentioned arm and then the free movement of the pendulum [16]. The arm's movement go through the horizontal plane and positive or negative angles can be obtained from that movement, representing its respective angular positions (θ_0), in radians, measured by an encoder, coupled to the motor's axle [7, 17, 18]. In the other arm's extremity, a potentiometer and a pendulum are coupled to it. In addition to the pendulum's angular position measurement (θ_1), this set also allows the free and oscillatory pendulum's movement, throughout the vertical plane. For a better understanding, the main considered parameters and variables of the rotary inverted pendulum are shown in Fig. 1.

In order to obtain the mathematical model of the rotary inverted pendulum, its several parameters are required. The considered parameters were obtained from a real system, under construction, available at the Automation Laboratory of the Federal Institute of Paraná (IFPR) – Jacarezinho – Paraná – Brazil, and they are presented in Tab. 1.

The moments of inertia of the system are individually obtained for the arm and pendulum's sets [7]. The junction between the arm and the pendulum is made by a potentiometer, whose its axis has a length of $l = 0.012$ m, a radius of $R = 0.003$ m and a mass of $m = 0.010$ kg.

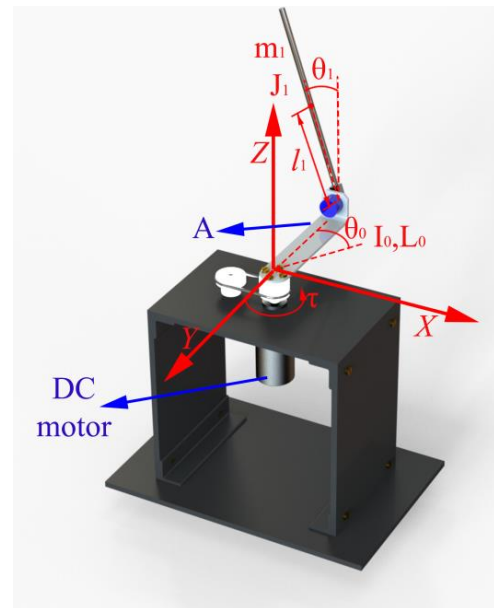


Fig. 1. Rotary inverted pendulum.

Tab. 1: Parameters of the rotary inverted pendulum.

Symbol	Description	Value	Unit
g	Gravitational acceleration	9.81	m/s ²
l_1	Distance between the half pendulum and the potentiometer	0.145	m
L_0	Distance between the arm's center and the potentiometer	0.150	m
m_1	Pendulum's mass	0.0248	kg
m_0	Arm's mass	0.155	kg

The presented parameters were used to calculate the inertia of the potentiometer axis, I_p :

$$I_p = \frac{1}{2} mR^2 = 4.5000 \times 10^{-8} \text{kg m}^2. \quad (1)$$

The inertia of the pendulum, I_H , is also necessary in the total inertia composition of the pendulum set, and using the data from Tab. 1, it is given by:

$$I_H = \frac{1}{12} m_1 (2l_1)^2 = 1.7381 \times 10^{-4} \text{kg m}^2. \quad (2)$$

The total inertia of the pendulum set, J_1 , is composed by the sum of the inertias from the potentiometer and the pendulum. From (1), (2), it is possible to compute:

$$J_1 = I_p + I_H = 0.00017385 \text{kg m}^2. \quad (3)$$

The same procedure is used to calculate the inertia of the arm's set, which is attached to one of the DC motor extremities (see Fig. 1). The main parameters from the DC motor considered in this work are presented in Tab. 2.

Tab. 2: Parameters of the DC motor.

Symbol	Description	Value	Unit
D	Diameter of the motor	0.036	m
r_M	Radius of the motor shaft	0.009	m
m_M	Mass of the motor	0.450	kg
m_r	Mass of the joint screw	0.005	kg

After obtaining the DC motor parameters (Tab. 2), it is possible to calculate the moment of inertia from the DC motor, I_M :

$$I_M = \frac{1}{2} \left(\frac{m_M}{2} + 0.005 \right) r_M^2 = 9.3150 \times 10^{-6} \text{ kg m}^2. \quad (4)$$

Moreover, (5) allow us to calculate the moment of inertia of the arm, I_B , using the parameters presented in Tab. 1:

$$I_B = \frac{1}{3} m_0 L_0^2 = 0.0012 \text{ kg m}^2. \quad (5)$$

Finally, the total inertia of the arm's set, I_0 , is obtained by the sum of I_M and I_B , and from (4) and (5), it follows:

$$I_0 = I_M + I_B = 0.001209315 \text{ kg m}^2. \quad (6)$$

III. MATHEMATICAL MODEL

The rotary inverted pendulum is composed by two bodies which interact with each other and then results in a combined movement between the pendulum (θ_1 angle in Fig. 1) and the arm (θ_0 angle in Fig. 1), since the last one connects the pendulum to the motor. In the mathematical modelling considered in this work, a linear approximation around an operation point of the pendulum system is considered. The operation point consists of the pair (x^*, u^*) , where x^* is the state of the system and u^* is the control signal. The non-linear model of the rotary inverted pendulum can be obtained through the Euler-Lagrange equations, which result in [7, 19, 20]:

$$M(q)\ddot{q} + C(q, \dot{q}) + g(q) = F \quad (7)$$

where

$$M(q) = \begin{bmatrix} M_{11}(q) & m_1 l_1 L_0 \cos(\theta_1(t)) \\ m_1 l_1 L_0 \cos(\theta_1(t)) & I_1 + m_1 l_1^2 \end{bmatrix},$$

$$M_{11}(q) = I_0 + m_1 (L_0^2 + l_1^2 \sin^2(\theta_1(t))),$$

$$C(q, \dot{q}) = \begin{bmatrix} C_{11}(q, \dot{q}) & C_{12}(q, \dot{q}) \\ C_{21}(q, \dot{q}) & 0 \end{bmatrix},$$

$$C_{11}(q, \dot{q}) = \frac{1}{2} m_1 l_1^2 \dot{\theta}_1(t) \sin(2\theta_1(t)),$$

$$C_{12}(q, \dot{q}) = -m_1 l_1 L_0 \dot{\theta}_1(t) \sin(\theta_1(t)) + \frac{1}{2} m_1 l_1^2 \dot{\theta}_0(t) \sin(2\theta_1(t)),$$

$$C_{21}(q, \dot{q}) = -\frac{1}{2} m_1 l_1^2 \dot{\theta}_0(t) \sin(2\theta_1(t)).$$

$$g(q) = \begin{bmatrix} 0 \\ -m_1 l_1 g \sin(\theta_1(t)) \end{bmatrix},$$

$$F = \begin{bmatrix} \tau \\ 0 \end{bmatrix}, q = \begin{bmatrix} \theta_0 \\ \theta_1 \end{bmatrix},$$

and τ represents the torque applied in the system by the DC motor. Thus, by isolating \ddot{q} in (7), (8) can be obtained:

$$\ddot{q} = M^{-1}(q)[-C(q, \dot{q})[x_2, x_4]^T - g(q) + F] = \begin{bmatrix} \omega_1(q, \dot{q}, \tau) \\ \omega_2(q, \dot{q}, \tau) \end{bmatrix}. \quad (8)$$

In order to obtain the state space model, the arm and the pendulum's angular positions, θ_0 and θ_1 , respectively, and their angular velocities, $\dot{\theta}_0$ and $\dot{\theta}_1$, were defined as state variables. Thus, from (8) and from the defined state variables, the non-linear model in the state space is achieved:

$$\begin{aligned} x &= [x_1 \ x_2 \ x_3 \ x_4]^T \\ &= [\theta_0 \ \dot{\theta}_0 \ \theta_1 \ \dot{\theta}_1]^T, \\ \dot{x} &= f(x, u) \\ &= \begin{bmatrix} f_1(x, u) \\ f_2(x, u) \\ f_3(x, u) \\ f_4(x, u) \end{bmatrix} = \begin{bmatrix} x_2 \\ \omega_1(x_1, x_2, x_3, x_4, u) \\ x_4 \\ \omega_2(x_1, x_2, x_3, x_4, u) \end{bmatrix}, \\ u &= \tau. \end{aligned} \quad (9)$$

In the Furuta pendulum, from the control systems point of view, the main objective is to keep the pendulum in the inverted position ($\theta_1 = 0$). For this objective, a linear approximation around the pair (x^*, u^*) , according (10), is considered. In this case, there is no initial condition for $x_1^* = \theta_0^*$, which means that this variable can be arbitrarily chosen, unlike the state variable $x_3^* = \dot{\theta}_1^* = 0$, that is, the pendulum must be close to the inverted position [7, 21, 22].

$$\begin{aligned} x^* &= [x_1 \ x_2 \ x_3 \ x_4]^T = [\theta_0^* \ 0 \ 0 \ 0]^T, \\ u^* &= 0, \\ \dot{x} &= f(x^*, u^*) = [0 \ 0 \ 0 \ 0]^T. \end{aligned} \quad (10)$$

The model (9) after being linearized around the equilibrium point (10) is given by [5]:

$$\begin{aligned} \dot{x} &= Ax + Bu, \\ y &= Cx, \quad z = C_T x, \end{aligned} \quad (11)$$

where

$$A = \begin{bmatrix} \frac{\partial f_1(x, u)}{\partial x_1} & \frac{\partial f_1(x, u)}{\partial x_2} & \frac{\partial f_1(x, u)}{\partial x_3} & \frac{\partial f_1(x, u)}{\partial x_4} \\ \frac{\partial f_2(x, u)}{\partial x_1} & \frac{\partial f_2(x, u)}{\partial x_2} & \frac{\partial f_2(x, u)}{\partial x_3} & \frac{\partial f_2(x, u)}{\partial x_4} \\ \frac{\partial f_3(x, u)}{\partial x_1} & \frac{\partial f_3(x, u)}{\partial x_2} & \frac{\partial f_3(x, u)}{\partial x_3} & \frac{\partial f_3(x, u)}{\partial x_4} \\ \frac{\partial f_4(x, u)}{\partial x_1} & \frac{\partial f_4(x, u)}{\partial x_2} & \frac{\partial f_4(x, u)}{\partial x_3} & \frac{\partial f_4(x, u)}{\partial x_4} \end{bmatrix},$$

$$B = \begin{bmatrix} \frac{\partial f_1(x, u)}{\partial u} \\ \frac{\partial f_2(x, u)}{\partial u} \\ \frac{\partial f_3(x, u)}{\partial u} \\ \frac{\partial f_4(x, u)}{\partial u} \end{bmatrix}.$$

Let x be the state vector, y the measured output vector and z the controlled output vector, A the state matrix, B the control input matrix, C the measured output matrix and C_T the controlled output matrix, in such way that the measured outputs are the angular positions, θ_0 and θ_1 , and the controllable output is the arm angle, θ_0 , thus

$$C = \begin{bmatrix} 1 & 0 & 0 & 0 \\ 0 & 0 & 1 & 0 \end{bmatrix}, \quad (12)$$

$$C_T = [1 \ 0 \ 0 \ 0].$$

Therefore, from (9) and (11), the state and control input matrices are:

$$A = \begin{bmatrix} 0 & 1 & \frac{-gm_1^2 l_1^2 L_0}{I_0(J_1 + m_1 l_1^2) + J_1 m_1 L_0^2} & 0 \\ 0 & 0 & 0 & 0 \\ 0 & 0 & 0 & 1 \\ 0 & 0 & \frac{(I_0 + m_1 L_0^2)m_1 l_1 g}{I_0(J_1 + m_1 l_1^2) + J_1 m_1 L_0^2} & 0 \end{bmatrix}$$

$$B = \begin{bmatrix} 0 \\ \frac{J_1 + m_1 l_1^2}{I_0(J_1 + m_1 l_1^2) + J_1 m_1 L_0^2} \\ 0 \\ \frac{-m_1 l_1 L_0}{I_0(J_1 + m_1 l_1^2) + J_1 m_1 L_0^2} \end{bmatrix}$$

and then, from the data in (3), (6) and Tab. 1,

$$A = \begin{bmatrix} 0 & 1 & 0 & 0 \\ 0 & 0 & -20.8703 & 0 \\ 0 & 0 & 0 & 1 \\ 0 & 0 & 66.9295 & 0 \end{bmatrix}, \quad (13)$$

$$B = \begin{bmatrix} 0 \\ 762.5775 \\ 0 \\ -591.6167 \end{bmatrix}.$$

It is important to notice that the model (11), (12) and (13) considers state vectors around the operation

point presented in (10), in which $\theta_1 = 0$, that is, the pendulum is in the vertical position (see Fig. 1). That means the swing-up control such that $\theta_1 = \pi$ changes to $\theta_1 = 0$ cannot be achieved with a controller which its design is based on the presented linear model. On the other hand, this problem can be solved using a controller which its design is based on a non-linear model of the plant [7].

IV. TRACKING SYSTEM CONTROLLER AND STATE OBSERVER

The tracking system controller with state feedback is designed by means of the linear model of the rotary inverted pendulum, as shown in (11), (12) and (13), aiming that the system output, $z(t)$, follows a desired input, $r(t)$, then the intended steady-state response is such that [14]:

$$\lim_{t \rightarrow \infty} z(t) = r(t). \quad (14)$$

The controller design methodology considers new state variables, $\xi(t)$, whose dynamics depend on the difference between the reference $r(t)$ and the system controlled output $z(t)$, as explained in [5], thus, from (11) and (12), ξ is defined as

$$\xi = r - z = r - C_T x. \quad (15)$$

The control law herein considered encompasses the plant state feedback, x , and the feedback of the new state variable ξ , therefore,

$$u = -Kx + K_I \xi. \quad (16)$$

A block diagram of the tracking system controller applied in the rotary inverted pendulum model is presented in Fig. 2, according to (11), (15) and (16).

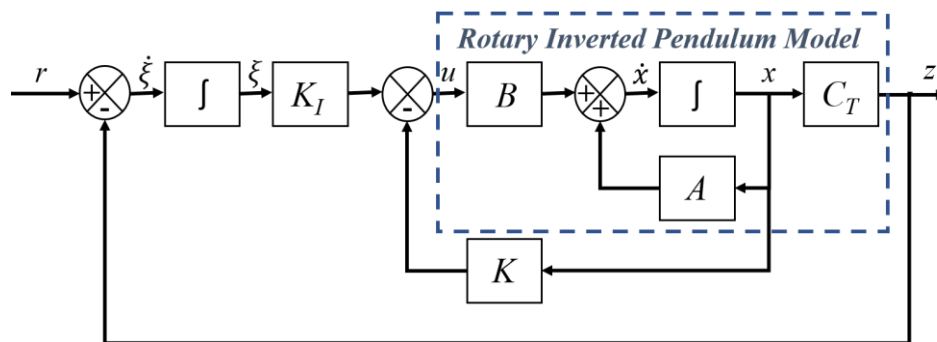


Fig. 2. Block diagram of the tracking system controller along with the rotary inverted pendulum model.

From (11), (15) and (16), the overall system is given by the augmented state equation, given by:

$$\begin{bmatrix} \dot{x}(t) \\ \dot{\xi}(t) \end{bmatrix} = \begin{bmatrix} A & 0 \\ -C_T & 0 \end{bmatrix} \begin{bmatrix} x(t) \\ \xi(t) \end{bmatrix} + \begin{bmatrix} B \\ 0 \end{bmatrix} u(t) + \begin{bmatrix} 0 \\ I \end{bmatrix} r(t), \quad (17)$$

where I represents the identity matrix of adequate dimension.

An asymptotically stable system is designed so that $x(\infty)$, $\xi(\infty)$ and $u(\infty)$ converge to constant values. So, during steady state, $\xi(t) = 0$, and then $z(\infty) = r$. Based on these definitions, from (17),

$$\begin{bmatrix} \dot{x}(\infty) \\ \dot{\xi}(\infty) \end{bmatrix} = \begin{bmatrix} A & 0 \\ -C_T & 0 \end{bmatrix} \begin{bmatrix} x(\infty) \\ \xi(\infty) \end{bmatrix} + \begin{bmatrix} B \\ 0 \end{bmatrix} u(\infty) + \begin{bmatrix} 0 \\ I \end{bmatrix} r(\infty). \quad (18)$$

Considering that $r(t)$ is a step input, so $r(\infty) = r(t) = r$ for $t > 0$. In this case, subtracting (18) from (17), one obtains:

$$\begin{bmatrix} \dot{x}_e(t) \\ \dot{\xi}_e(t) \end{bmatrix} = \begin{bmatrix} A & 0 \\ -C_T & 0 \end{bmatrix} \begin{bmatrix} x_e(t) \\ \xi_e(t) \end{bmatrix} + \begin{bmatrix} B \\ 0 \end{bmatrix} u_e(t),$$

$$\begin{aligned} x_e(t) &= x(t) - x(\infty), \\ \xi_e(t) &= \xi(t) - \xi(\infty), \\ u_e(t) &= u(t) - u(\infty), \end{aligned} \quad (19)$$

where $u_e(t)$ is defined by:

$$\begin{aligned} u_e(t) &= -Kx_e(t) + K_I \xi_e(t) \\ &= -[K \quad -K_I] \begin{bmatrix} x_e(t) \\ \xi_e(t) \end{bmatrix}. \end{aligned} \quad (20)$$

Assuming the new error vector $e(t) = [x_e(t)^T \quad \xi_e(t)^T]^T$, from (19) and (20), the following dynamics is obtained:

$$\begin{aligned} \dot{e} &= (\hat{A} - \hat{B}\hat{K})e, \\ \hat{A} &= \begin{bmatrix} A & 0 \\ -C_T & 0 \end{bmatrix}, \quad \hat{B} = \begin{bmatrix} B \\ 0 \end{bmatrix}, \\ \hat{K} &= [K \quad -K_I], \end{aligned} \quad (21)$$

then the gain matrix \hat{K} must be designed so that the dynamics (21) be stable.

Considering $z(t) \in \mathfrak{R}$ from (11), if the desired eigenvalues of the matrix $\hat{A} - \hat{B}\hat{K}$ are defined by l_1, l_2, \dots, l_{n+1} , then the state feedback gain matrix K and the integral gain constant K_I can be designed by the pole placement method, whenever the system (21) be a fully state controllable system [5].

The eigenvalue vector considered in the tracking system controller design by pole placement was

$$l = [-3 \quad -4 \quad -5 \quad -6 \quad -7], \quad (22)$$

which resulted in the following gains for the tracking control system of the rotary inverted pendulum:

$$\hat{K} = [K \quad -K_I], \quad (23)$$

$$\begin{aligned} K &= [-0.0712 \quad -0.0317 \quad -0.619 \quad -0.0831] \\ K_I &= [-0.0651]. \end{aligned}$$

In general, the control using state feedback strategies assumes that all state variables can be measured, or they can be generated from the output system. For practical issues, this fact can be unfeasible, due to the number of sensors required for that measurements. Then, for the state variables estimation from the plant output $y(t)$ in (11), a state observer is considered in this work. It is important to notice that the system (11) with output $y(t)$ is observable [14].

An observer is a dynamical system which estimates the plant state vector. It can be designed independently of the tracking system controller (15) and (16) by using pole placement techniques [5]. The mathematical models from the observer system and the plant system are similar, except by adding a term that encompasses the estimated error, in order to compensate uncertainties from the matrices A and B of the plant model, and the possible initial condition error.

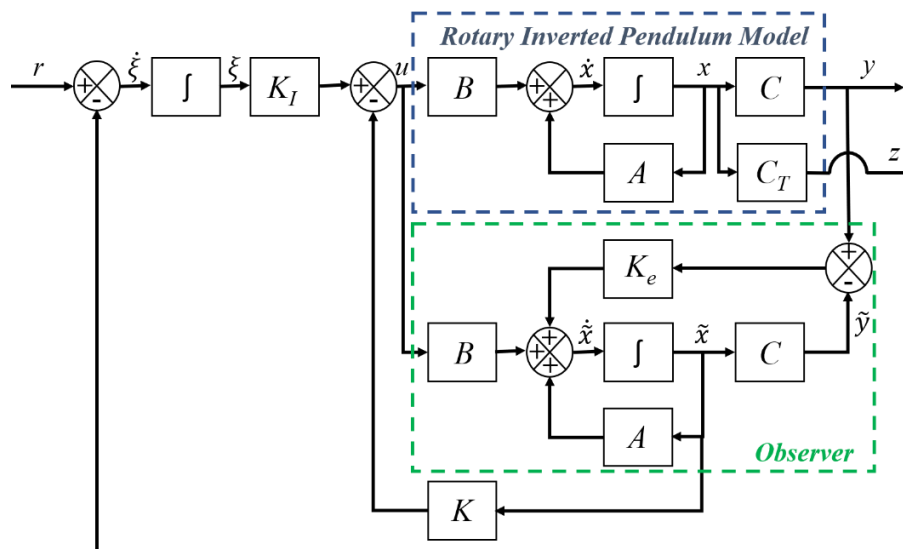


Fig. 3. Block diagram of the tracking system controller along with the rotary inverted pendulum model and the state observer.

The initial condition error is the difference between the initial state from the plant and the estimated initial state from the observer.

Therefore, the mathematical model of the observer is given by [5]:

$$\begin{aligned} \dot{\tilde{x}} &= A\tilde{x} + Bu + K_e(y - C\tilde{x}) \\ &= (A - K_eC)\tilde{x} + Bu + K_e y, \end{aligned} \quad (24)$$

where \tilde{x} and $C\tilde{x}$ are the estimated state vector and output, respectively. The observer's inputs are the plant output, y , and the control signal, u . The K_e matrix is called the observer's gain matrix, and it ponders the difference between the measured output, y , and the estimated output, $C\tilde{x}$. Therefore, the observer is able to correct the state estimative and

then provides a good performance [5]. In Fig. 3, the use of the tracking system controller along with state observer in the inverted pendulum model is illustrated.

In order to obtain the observation error $e = x - \hat{x}$, (24) is subtracted from (11), what results in

$$\begin{aligned} \dot{e} = \dot{x} - \dot{\hat{x}} &= Ax - A\hat{x} - K_e(Cx - C\hat{x}) \\ &= (A - K_eC)(x - \hat{x}) \\ &= (A - K_eC)e. \end{aligned} \quad (25)$$

The eigenvalues from $(A - K_eC)$ are defined so that they are at left from the eigenvalues of the $(\hat{A} - \hat{B}\hat{K})$ in (21). Then, if the state observer presents an initial error in relation to the plant initial condition, this error will tend to zero as the time increases [5]. The eigenvalue vector L were used in the observer design for the rotary inverted pendulum, using a pole placement technique, where

$$L = [-15 \quad -20 \quad -25 \quad -30]. \quad (26)$$

The obtained observer's gain matrix K_e were

$$K_e = \begin{bmatrix} 46.6436 & -4.8535 \\ 525.0847 & -130.3134 \\ -4.5920 & 43.3564 \\ -102.6790 & 516.8332 \end{bmatrix}. \quad (27)$$

V. RESULTS AND DISCUSSION

The results presented in this section are organized in two simulation cases:

Case 1: only the tracking system controller, gain matrix (23);

Case 2: tracking system controller along with the state observer, gain matrices (23) and (27).

The first set of simulations begins with the pendulum around the inverted position, with $\theta_1 = \pi/6$ rad, that is, $x(0) = [0 \quad 0 \quad \pi/6 \quad 0]^T$. The simulation results, under this defined initial condition, are presented in Fig. 4, the control inputs, and Figs. 5 and 6, the state variables. It is possible to notice that, in both Case 1 and Case 2, the control strategies lead the system to the equilibrium point.

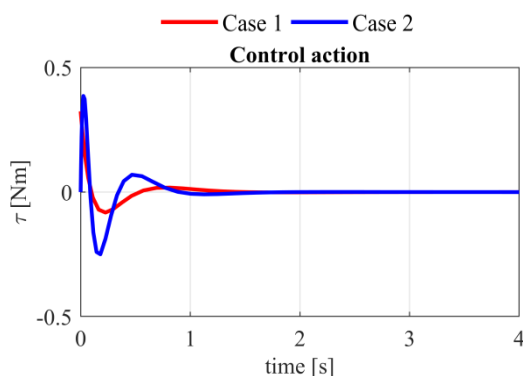


Fig. 4. Control signals from the simulations with $x(0) = [0 \quad 0 \quad \pi/6 \quad 0]^T$.

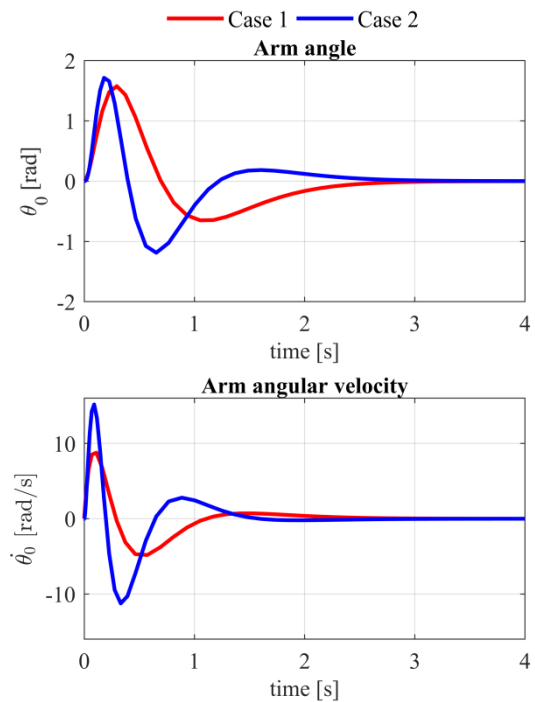


Fig. 5. Angular position and angular velocity of the arm movement from the simulations with $x(0) = [0 \quad 0 \quad \pi/6 \quad 0]^T$.

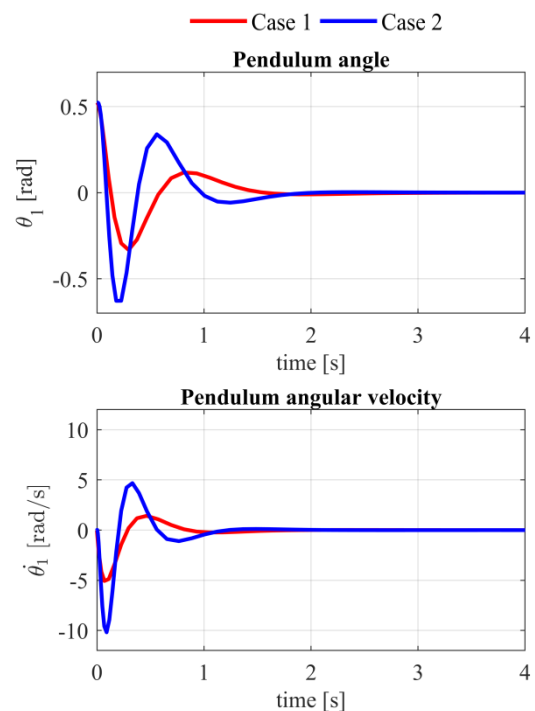


Fig. 6. Angular position and angular velocity of the pendulum movement from the simulations with $x(0) = [0 \quad 0 \quad \pi/6 \quad 0]^T$.

Furthermore, it can be observed that, both state variables (Fig. 5 and Fig. 6) and control signal (Fig. 4), are distinct between Case 1 and Case 2.

That difference is due to the null initial condition in the observer, while the plant has a non-null initial condition. However, this fact did not result in a system instability in any case.

In order to verify if the tracking system controller is able to make the controlled output z follow a desired reference r , after the pendulum stabilization at the equilibrium point $x(0) = [0 \ 0 \ 0 \ 0]^T$, the second set of simulation considers reference, $r(t)$ applied to the controlled system. This reference changes from $r = 0$ to $r = \pi/12$ rad, at the instant 1 s, then it maintains this value till it returns to zero at the time 5 s. The control signals and the state variables in this scenario are presented in Figs. 7, 8 and 9, respectively. The presented control system performance highlights the efficacy of the strategies.

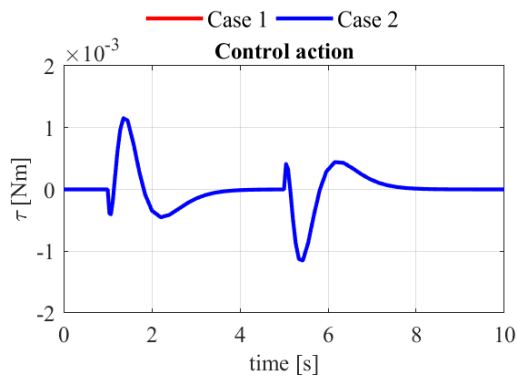


Fig. 7. Control signals from the simulations with a reference (in Fig. 8) for the arm angle θ_0 .

It is important to observe that the control strategies, in both considered cases (Case 1 and Case 2), provide similar responses in the second set of simulations. That similarity in the Figs. 7, 8 and 9 is due to the initial state from the observer and from the plant were equal (null) in the beginning of the simulations, when the system is considered in the equilibrium point.

VI. CONCLUSION

This work presented control methodologies for a rotary inverted pendulum system (Furuta pendulum). The used control strategies considered the linearization from the non-linear model of the plant around an equilibrium point, which was the predefined position for the system stabilization (inverted position). From this point, the main objective of the methodologies was to keep the angular position of the pendulum at 0 rad, so that the inverted position is maintained.

From the initial simulation results, it is possible to conclude that the proposed tracking system control methodology with state feedback was efficient in achieving the control objective, because

the controller was able to make the arm angular position follow a required reference, as well as to stabilize the pendulum at the desired position.

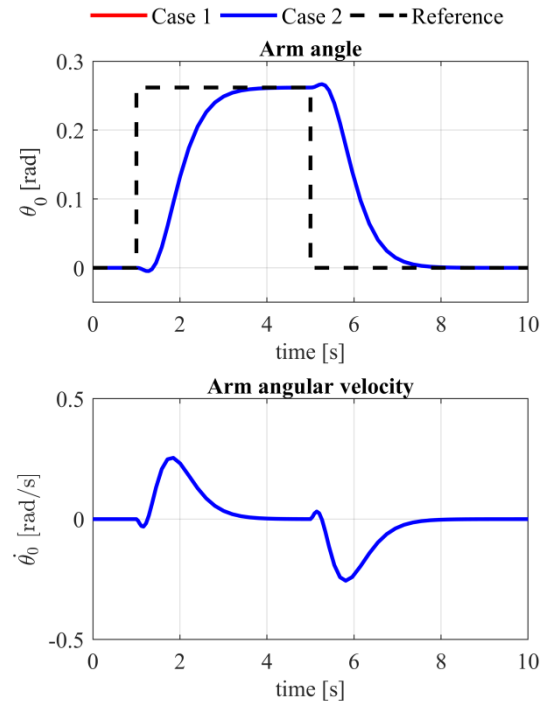


Fig. 8. Angular position and angular velocity of the arm movement from the simulations with a reference for the arm angle θ_0 .

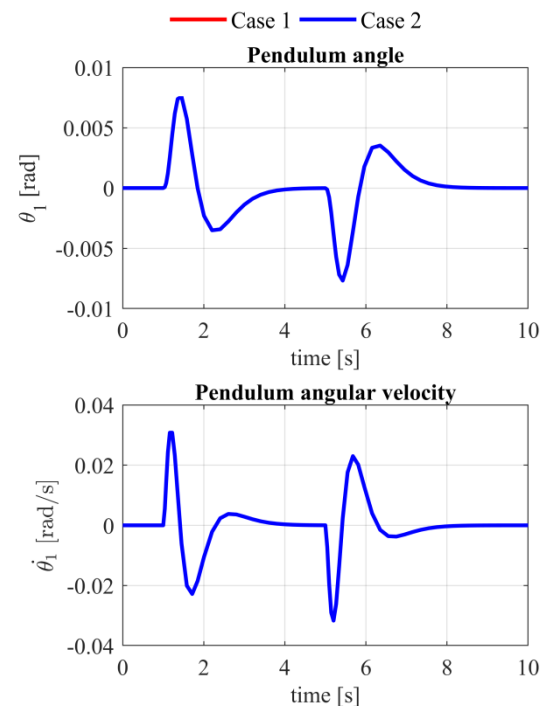


Fig. 9. Angular position and angular velocity of the pendulum movement from the simulations with a reference (in Fig. 8) for the arm angle θ_0 .

The second methodology used a state observer to estimate the plant's state vector, the results in this case show it is a valid option when there are no sensors for all the state variable measurements.

The tracking system controller along with the observer used in the plant resulted in a more oscillatory response compared with the use of the state feedback. It occurs whenever there are different initial conditions in the observer and in the plant. However, this strategy was also able to stabilize the pendulum, which means it is a valid approach for the control of a rotary inverted pendulum.

For future works, the authors intend to obtain experimental results from a real rotary inverted pendulum, at the Automation Laboratory of the IFPR, in order to validate the mathematical model and the approached control strategies from this paper.

ACKNOWLEDGEMENTS

The authors would like to thank to the Federal Institute of Paraná, Jacarezinho, for supporting the development of this work.

REFERENCES

- [1]. K. Furuta, M. Yamakita, S. Kobayashi, Swing-up control of inverted pendulum using pseudo-state feedback, *Journal of Systems and Control Engineering*, 206(6), 1992, 263–269.
- [2]. K.J. Astrom, K. Furuta, Swinging up a pendulum by energy control, *Automatica*, Elsevier, 2000, 287-295.
- [3]. M. Yamakita, T. Hooshino, K. Furuta, Control Practice Using Pendulum, *Proceedings of the American Control Conference*, San Diego, California, 1999.
- [4]. M. Furka, M. Klauco, M. Kvasnica, Stabilization of Furuta Pendulum using Nonlinear MPC, *Research Papers Faculty of Materials Science and Technology in Trnava, SCIENDO*, vol27, number45, Bratislava, 2019, 42-48.
- [5]. K. Ogata, *Modern Control Engineering*, Pearson Prentice Hall, 4 ed, São Paulo, 2007, 695-710.
- [6]. P. Seman, B. Rohal-Ilkiv, M. Juhás, M. Salaj, Swinging up the Furuta Pendulum and its Stabilization via model Predictive Control, *Journal of Electrical Engineering*, vol.64, n.3, 2013, 152-158.
- [7]. V.M.H. Guzmán, M.A. Cruz, R.S. Ortigoza, Linear State Feedback Regulation of a Furuta Pendulum: Design Based on Differential Flatness and Root Locus, *Special Section on Innovations In Electrical and Computer Engineering Education*, vol 4, 2016, 8721-8736.
- [8]. J.S. Sham, M.I.F. Solihin, Heltha, H. Muzaiyanah, Modelling and Simulation of an Inverted Pendulum System: Comparison Between Experiment and Cad Physical Model, *ARPJ Journal of Engineering and Applied Sciences*, vol. 10, n. 20, 2015, 9752-9757.
- [9]. Xiumin Diao, Modular Control of a Rotary Inverted Pendulum System, *American Society for Engineering Education, Conference & Exposition*, New Orleans, 123rd Annual, 2016, pp- 1-15.
- [10]. S. Jadlovska, J. Sarnovsky, A Complex Overview of Modeling and Control of the Rotary Single Inverted Pendulum System, *Power Engineering and Electrical Engineering*, vol.11, n.2, 2013, 73-85.
- [11]. Y. Beceriklia, B.K. Celik, Fuzzy control of inverted pendulum and concept of stability using Java application, *Mathematical and Computer Modeling*, 2007, 4624–37.
- [12]. A. Jain, D.T.N. Sehgal, Control of Non-Linear Inverted Pendulum using Fuzzy Logic Controller. *International Journal of Computer Applications*, (0975 – 8887) vol 69, n.27. 2013.
- [13]. Shadab Khan, S. Paliwal, Optimal Control of Nonlinear Inverted Pendulum System Using fuzzy controller, *International Journal of Engineering Research and Applications (IJERA)*, vol. 8, no.5, 2018, 62-66
- [14]. J.J. D'azzo, and H.C. Houppis, *Linear Control System Analysis and Design: Conventional and Modern*, McGraw Hill, New York, 1995, 651-659.
- [15]. R. Breganon, M.M. Souza, F.T.B. Salvi, R.C. Lemes, M.A.F. Montezuma, E. M. Belo, Attitude and Position Tracking System for a 6-6 Stewart Platform, In: *22nd International Congress of Mechanical Engineering*, 2013, Ribeirão Preto.
- [16]. G.T. García, J.T. Buitrago, J.M. Ramírez, Control and friction of Furuta pendulum, state of art, *Scientia et Technical*, vol. 20, n. 4, 2015, 326- 334.
- [17]. Olfa Boubaker, The Inverted Pendulum Benchmark in Nonlinear Control Theory: A Survey, *International Journal of Advanced Robotic Systems*, vol. 10, 2013, 1-9.
- [18]. M.R. Hamers, Revitalizing the Furuta pendulum, *DCT rapporten, Eindhoven Technische*, Universiteit Eindhoven, vol. 099, 2004.
- [19]. J.Á. Acosta, Furuta Pendulum: A Conservative Nonlinear Model for Theory

- and Practice, Mathematical Problems in Engineering, Hindawi Publishing Corporation, 2010, 1-30.
- [20]. N. Gupta, L. Dewan, Modeling and simulation of rotary-rotary planer inverted pendulum, *IOP Conf. Series: Journal of Physics*: 1240, 2019, 1-9.
- [21]. B.S. Cazzolato, Z. Prime, On the Dynamics on the Furuta Pendulum, *Journal of Control Science and Engineering*, Hindawi Publishing Corporation, 2011,1-8.
- [22]. O.O.R. Díaz, E.L.T. Valderrama, D.A.G. Ramirez, Simulating a Rotational Inverted Pendulum Model by using Matlab and Easy Java Simulations, *Rev. Tecno Lógicas*, n.28, 2012, 15-32.

Luiz Eduardo Pivovar, et. al. "A Tracking System Control Approach Applied on a Rotary Inverted Pendulum Model." *International Journal of Engineering Research and Applications (IJERA)*, vol.10 (06), 2020, pp 48-56.